FLUORESCENCE EMISSION SPECTROSCOPY OF 1,4-DIHYDROXYPHTHALONITRILE

A Method for Determining Intracellular pH in Cultured Cells

IRA KURTZ AND ROBERT S. BALABAN
National Heart, Lung and Blood Institute, Laboratory of Kidney and Electrolyte Metabolism,
Bethesda, Maryland 20205

ABSTRACT   We have developed new methodology for measuring intracellular pH (pH_i) in cultured cell monolayers and epithelia by analyzing the emission spectra of the trapped fluorescent pH probe, 1,4-dihydroxyphthalonitrile (1,4-DHPN). This compound is unique since both its acid and base forms possess different fluorescence emission characteristics that can be used to quantitate pH_i. The fluorescence difference spectrum between an acid and alkaline solution of 1,4-DHPN has a maximum at 455 nm and a minimum at 512 nm. By determining the ratio of the intensity at these two wavelengths as a function of pH, a calibration curve was constructed. Since the two intensities are determined simultaneously, the measurement is independent of dye concentration, bleaching, and intensity fluctuation of the excitation source. Furthermore, analysis of the emission spectra permitted the detection of light scattering, binding effects, and chemical modification of the probe. A microspectrofluorometer was constructed to analyze low light level emission spectra from intracellular 1,4-DHPN. The instrument consists of a modified Leitz inverted microscope (E. Leitz, Inc., Rockleigh, NJ) with a Ploem illuminator adapted for broadband excitation and objective focusing capability. The emission spectra were collected by focusing the fluorescence from the cell onto the entrance slit of an imaging monochromator, which was scanned by a SIT camera interfaced with a computer. This permitted the acquisition of fluorescence emission spectra extending from 391–588 nm in ~33 ms. pH_i measured in the cultured toad kidney epithelial cell line, A6, was 7.49 ± 0.04 ($n = 12$) with an external pH of 7.6. A6 cells were found to regulate pH_i in response to both acute acid and alkali loads and maintained pH_i relatively constant over a wide range of external pH values. The technique described in this report overcomes several of the difficulties encountered with other fluorescent pH probes where excitation spectroscopy is required to monitor pH.

INTRODUCTION

Intracellular pH (pH_i) is believed to play a central role in the regulation of numerous cellular phenomena (1, 2). Of the several methods available to determine pH_i, optical methods have several advantages including a rapid response time, high signal-to-noise ratio, and excellent pH sensitivity. The first use of a trapped intracellular pH probe 6-carboxyfluorescein (6-CF) was described in 1979 by Thomas et al. (3, 4). In this study Ehrlich acites cells were exposed to the lipid soluble compound 6-carboxy-fluorescein diacetate, which after permeating the plasma membrane was cleaved by intracellular esterases to the relatively impermeant derivative 6-CF. Excessive dye leakage out of cells and a low pK of ~6.3 have prompted the development of numerous analogues that have lower leak-

age rates and pK values that more closely approximate pH_i (5–8).

Despite these improvements, difficulties with the method still exist. The fluorescent excitation ratio method (7, 9, 10), a method used to correct for changes in dye concentration during the course of an experiment, requires that the fluorescent intensity at two excitation wavelengths (peak excitation and isosbestic excitation wavelengths) be measured separately in time such that bleaching, fluctuation in the intensity of the excitation source and dye leakage out of the cell, can alter the ratio of the two intensities independent of pH changes, and need to be compensated for. The intracellular excitation spectra of 6-CF and its analogues are red-shifted relative to the in vitro excitation spectra precluding the use of an in vitro calibration curve to quantitate pH_i (3, 5). Calibration of the intracellular fluorescence intensity as a function of pH_i is obtained indirectly using a compound such as the K^+/H^+ ionophore nigericin (3, 5) or a large excess of a weak acid or base to equilibrate the intracellular and extracellular pH (7). Many of the new analogues have

been loaded into cells by injection (7, 9) or osmotic lysis (8). These loading techniques can potentially perturb the intracellular milieu. Finally, pH_i measurements have been made using trapped fluorescence probes on cell suspensions studied in a cuvette placed in a standard spectrofluorometer (11–12). Although this approach offers the advantage of studying large numbers of cells, which increases the signal-to-noise ratio and decreases the single cell bleaching rate, there are difficulties with this technique such as (a) dye leakage into the extracellular medium, which contributes to the total fluorescence intensity, (b) scattering artifacts, (c) difficulty in analyzing intercellular or intracellular pH differences, and (d) possible anatomical and physiological alterations of the cells induced by forming a suspension from cells that are normally configured as an epithelium or grown attached to a substrate.

These limitations have prompted the development of an alternative method for monitoring pH_i in single living cells. Using the fluorescent pH probe 1,4-dihydroxyphthalonitrile (13, 14, 15) and a microspectrofluorometer, which was designed to rapidly acquire both spectral and topographical information from single cells, pH_i was monitored in cultured A6 monolayers derived from the kidney of the toad *Xenopus laevis* (16).

METHODS AND MATERIALS

Cells

A6 cells were obtained from American Tissue Culture Collection (Rockville, MD). Cells from passage 74 to 86 were grown in specially designed chambers (Fig. 1). The cells were incubated for ~7 d before study in CL-2 medium with the addition of penicillin (62 μg/ml), streptomycin (135 μg/ml), glutamine (0.3 mg/ml), and 10% fetal bovine serum. This medium was equilibrated with a gas mixture of 1% CO_2/99% O_2.
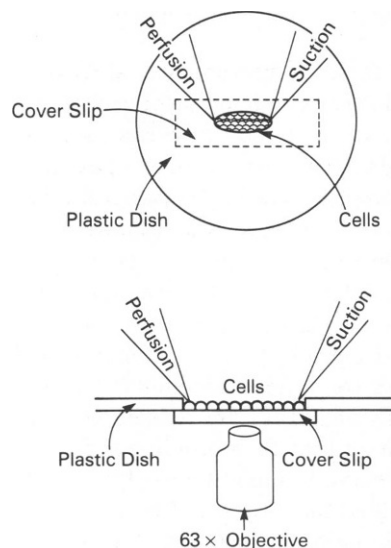
FIGURE 1   Chamber designed for growing and studying cultured cell monolayers.

1,4-Dihydroxyphthalonitrile

1,4-Dihydroxyphthalonitrile (1,4-DHPN) and the membrane permeant derivative 1,4-diacetoxyphthalonitrile (1,4-DAPN) were purchased from Molecular Probes, Inc. (Junction City, OR). The excitation and emission spectra of 1,4-DHPN at various pH values were obtained with an Aminco-Bowman spectrofluorometer (Urbana, IL) using 10 nm slit widths at 22°C. Spectra were obtained in a solution that was designed to simulate the intracellular milieu: HEPES (10 mM), Mes (10 mM), KCl (130 mM), NaCl (20 mM), KH_2PO_4 (10 mM), $MgCl_2 \cdot 6H_2O$ (1mM), 1,4-DHPN (0.1 mM); solution A. pH was measured with a glass universal pH electrode (Fisher Scientific Co., Allied Corp., Pittsburgh, PA) and an ion/pH 9000 meter (Sargent-Welch Co., Skokie, IL) before collection of the spectra. HEPES and Mes were purchased from Sigma Chemical Co. (St. Louis, MO)

Loading Cells

1,4-DAPN, the membrane permeant derivative of 1,4-DHPN, enters cells rapidly and is cleaved by intracellular esterases (and by nonenzymatic hydrolysis) to the relatively impermanent compound 1,4-DHPN (Fig. 2).

A stock solution of 1,4-DAPN was prepared on the day of study by dissolving 1.2×10^{-2} mM of 1,4-DAPN in 70 μl of dimethylsulphoxide (Sigma Chemical Co.) 6 μl of the stock solution was diluted in 4 ml of a solution that contained glucose (5 mM), NaCl (110 mM), KCl (3 mM), KH_2PO_4 (1 mM), $CaCl_2$ (1mM), $MgSO_4$ (0.5 mM), HEPES (10 mM) (pH 7.0); solution B. This solution was equilibrated with 100% O_2. The final concentration of 1,4-DAPN was 2.6×10^{-4} M; the final dilution of dimethylsulphoxide was 1:667 (vol/vol). On the day of a study, the chamber containing the monolayer of A6 cells was removed from the incubator and placed on the microspectrofluorometer stage. Solution B was used to rinse off the growth medium. The cells were then bathed in solution B for ~20 min at 22°C. Since the initial rate of nonenzymatic hydrolysis of 1,4-DAPN increases with pH, as has been demonstrated with other esterified probes (17), loading of 1,4-DAPN into the cells was performed at pH 7.0. Intracellular hydrolysis of 1,4-DAPN was detected by observing the change in its emission spectral properties (Fig. 3, A–C). After the 20-min loading period, solution B was rinsed off, and the solution bathing the monolayer was continually exchanged using a perfusion and suction system (Fig. 1). The rapid exchange of the bathing solution prevented dye, which had leaked out of the cells, from contributing to the measured fluorescence. Measurements could be obtained from stained A6 cells (Fig. 4) for 1–2 h.
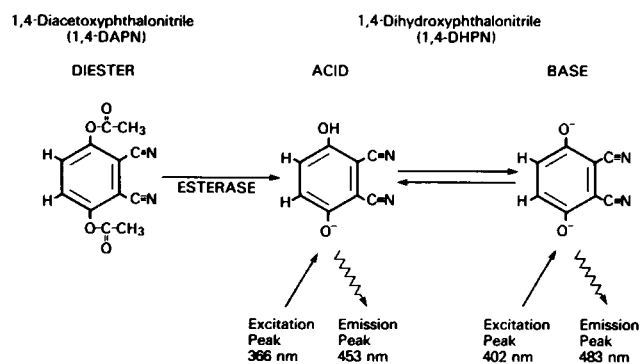
FIGURE 2   1,4-DAPN is a permeant diester that enters cells rapidly and is subsequently cleaved by cellular esterases. The product, 1,4-DHPN is relatively impermeable and fluoresces both in its acid (453 nm) and base forms (483 nm). The excitation maxima are corrected for the spectral output of the xenon light source and the emission maxima are corrected for the spectral sensitivity of the photomultiplier.
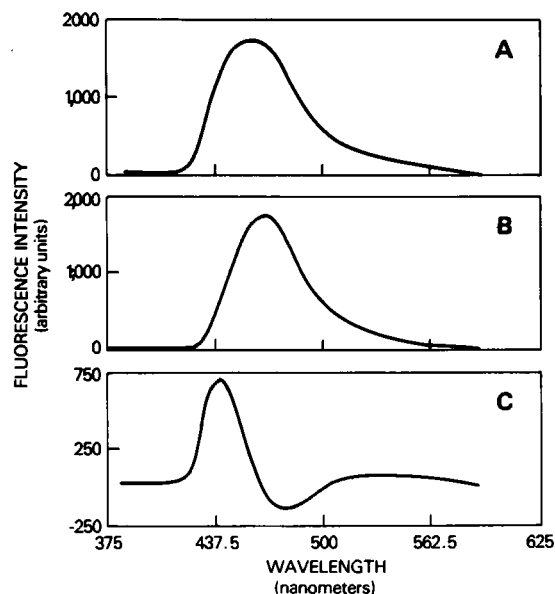
FIGURE 3 (*A*) Emission spectrum of 2.6×10^{-4} M 1,4-DAPN, HEPES buffered solution, pH 7 (55 scans) (*B*) Emission spectrum of 2.6×10^{-4} M 1,4-DHPN, HEPES buffered solution, pH 7 (1 scan). (*C*) Difference spectrum. As 1,4-DAPN is hydrolyzed to 1,4-DHPN the peak fluorescence intensity increases ~55 times (using 375–407 nm excitation light). In addition to the increase in intensity, there is a change in the shape of the emission spectrum. To compare the spectral shape of the two compounds, 55 scans of 1,4-DAPN (Fig. 3 *A*) and 1 scan of 1,4-DHPN (Fig. 3 *B*) were acquired so that the intensities of the spectra would be comparable. Fig. 3 *C* reveals the difference in spectral shape between the two compounds. Both the increase in fluorescence intensity and the change in spectral shape are used to detect the hydrolysis of 1,4-DAPN to 1,4-DHPN.

Multichannel Imaging Microspectrofluorometer

The microspectrofluorometer used in this study was designed to permit the rapid detection and analysis of low light level fluorescence emission or absorption spectra from living cells (Fig. 5). The apparatus consists of a Leitz inverted microscope (E. Leitz, Inc.), which was modified to permit the simultaneous acquisition of both topographic and spectral information. Fluorescence excitation of the cells was performed by focusing a collimated beam of light from a 75 W xenon arc lamp (Oriel Corp., Stamford, CT) onto a Ploem illuminator (E. Leitz, Inc.), which was modified for objective focusing capability. A custom excitation filter (transmission 375–407 nm) and dichroic mirror (reflectance 340–400 nm) purchased from Andover Corp. (Lawrence, MA), and a Leitz blocking filter, LP430 long pass filter with a 50% transmission at 450 nm, were inserted in an empty Leitz filter cube (E. Leitz, Inc.) and placed in the Pleom illuminator. An electronic shutter (A.W. Vincent Assoc., Rochester, NY) under computer control exposed the cells to the excitation source only during the collection of fluorescent spectra in order to minimize bleaching and photodamage. A Zeiss 63× Neofluar oil immersion long working distance objective (NA 1.25; Carl Zeiss, Inc.) was used in all the studies to both focus the excitation light onto the cells and to collect spectral and topographic information (epifluorescence).

Detector. The fluorescent image was focused by a Leitz 10× eyepiece (E. Leitz, Inc.) onto the proximal end of a randomly distributed fiber optic bundle. The distal end of the fiber bundle was coupled to a UFS 200 flat field imaging monochromator (Instruments SA, Inc., Metuchen, NJ). The output of the monochromator was imaged by a silicon intensified (SIT) vidicon (model 1254; EG&G Princeton Applied Research, Princeton, NJ). The SIT camera has a 12.5 × 12.5 mm active surface comprising 512 × 512 pixels. This resulted in the dispersion of a spectrum from 391 to 588 nm across ~500 channels (one channel defined as a number of pixels in the vertical direction) providing a spectral resolution of ~0.4 nm/channel.

To permit the simultaneous acquisition of topographic information from the cells, a second SIT camera (COHU INC, Model 4400, San Diego, CA) was mounted on the trinocular head of the microscope. The
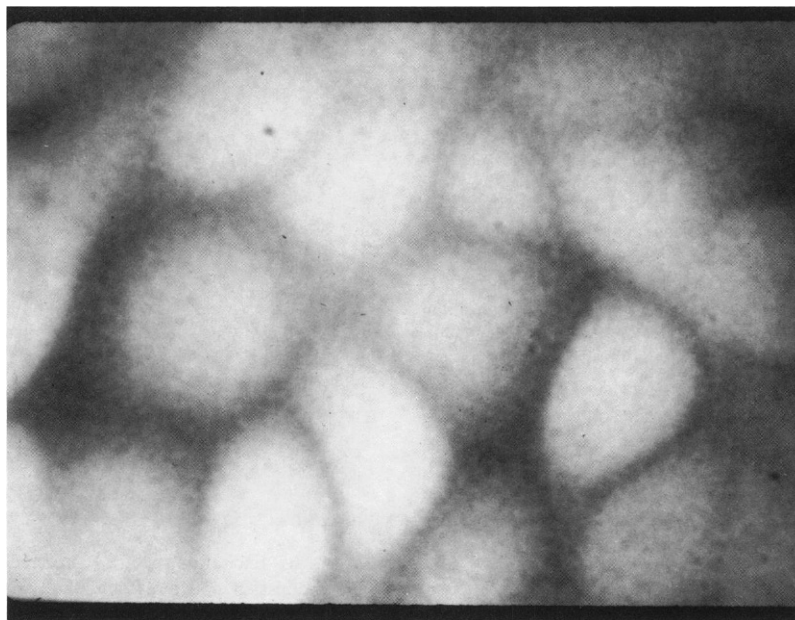

FIGURE 4 A6 cells stained with 1,4-DAPN. Note the diffuse staining of the cells indicating the lack of extensive compartmentation.
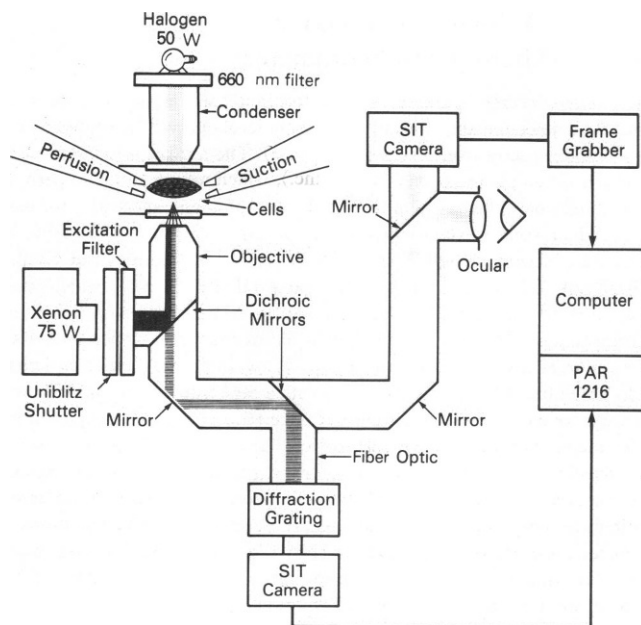
FIGURE 5 Microspectrofluorometer designed for acquiring low light level emission and absorption spectra from cultured cell monolayers. ■ represents excitation light (375–407 nm) that is reflected by the dichroic mirror to the tissue ▤ represents the fluorescence emission from the tissue that is transmitted by the same dichroic mirror and then reflected by a second dichroic mirror to the diffraction grating for spectral analysis. ▣ represents 660-nm light that is transmitted through both dichroic mirrors for observation of the tissue. The dichroic mirrors are interchangeable to permit the use of other probes with different spectral characteristics. In addition, the dichroic mirror immediately proximal to the diffraction grating can be removed completely to permit the direct observation of the fluorescence by eye or the SIT camera attached to the trinocular.

images from this camera were digitized in 1/30 s with a frame grabber (512 × 512 × 8 bits) purchased from Imaging Technology Inc. (Wolburn, MA). The cells were also observed visually during the course of an experiment under transmitted 660-nm light by placing a 660-nm bandpass filter in front of a 50-W tungsten-halogen lamp. A Leitz dichroic mirror (TK580 transmission 600–700 nm; E. Leitz, Inc.) placed in the base of the microfluorometer transmitted the 660-nm light to the trinocular for topographic analysis and reflected the 391–588 nm fluorescence to the monochromator for spectral analysis.

    Computer Interface. The scan pattern of the model 1254 SIT camera was controlled using a vidicon controller (model 1216; EG&G Princeton Applied Research), which was interfaced with a DECLAB 11/23 MINC minicomputer (Digital Equipment Corp., Marlboro, MA). The 1216 controller is a 16-bit programmable computer designed to digitize analog data from the 1254 SIT camera and provide scanning control. It contains a 14-bit analog-to-digital converter, a vidicon alignment board, a frame buffer that provides the scanned pixel locations, and a timing and control board to ensure proper sequencing. A series of 16-bit parallel function codes is sent from the minicomputer to the 1216 controller to determine the desired scan pattern of the 1254 SIT camera. In addition the minicomputer converts analog output from the 1216 controller to digital form for data analysis and storage. Data were displayed on a VT105 terminal (Digital Equipment Corp.) and was stored on either floppy or hard disk.

Data Acquisition

The multichannel imaging spectrometer is capable of acquiring an emission spectrum from 391–588 nm in 33 ms. The following sequence

was used to acquire spectra from the cells to eliminate the influence of changes in the dark current of the camera. First, scans of the dark current spectrum (produced by thermally generated current and scan-induced current) were collected and summed by the computer. An electronic shutter positioned in front of the xenon arc lamp opened and scans of the fluorescence emission from intracellular 1,4-DHPN were collected and summed. The shutter was closed under computer control immediately after the fluorescence emission spectra were collected. An equal number of scans were collected with and without the shutter open. The dark current spectrum was then digitally subtracted from the spectrum of 1,4-DHPN. The subtraction spectrum was displayed on a VT105 terminal (Digital Equipment Corp.) and was permanently stored for further analysis. The intensity of the cell autofluorescence from 391–588 nm was not different from zero (given the excitation wavelengths and number of scans, two per measurement, used in this study), precluding the need to subtract the autofluorescence spectrum from the intracellular 1,4-DHPN spectrum. Seven adjacent vidicon channels were averaged (~2.8 nm bandwidth) when assessing the fluorescence intensity at a desired wavelength. Programs for collection and analysis of the spectra were written in BASIC and are available from the authors on request. All values are reported as the mean ± standard error of the mean.

RESULTS

Fluorescence Excitation and Emission Spectra of 1,4-DHPN

Figs. 6 and 7 illustrate the fluorescence excitation and emission spectra of 1,4-DHPN in solution A (see methods for composition) at various pH values. The excitation spectra were corrected for the wavelength-dependent alteration in the xenon arc lamp intensity. The excitation peak shifts from 342 to 402 nm as pH is varied from 3 to 10 (emission measured at 470 nm). The fluorescence emission spectrum of 1,4-DHPN demonstrates a pH dependent shift in its emission maximum from 453 to 483 nm as pH is
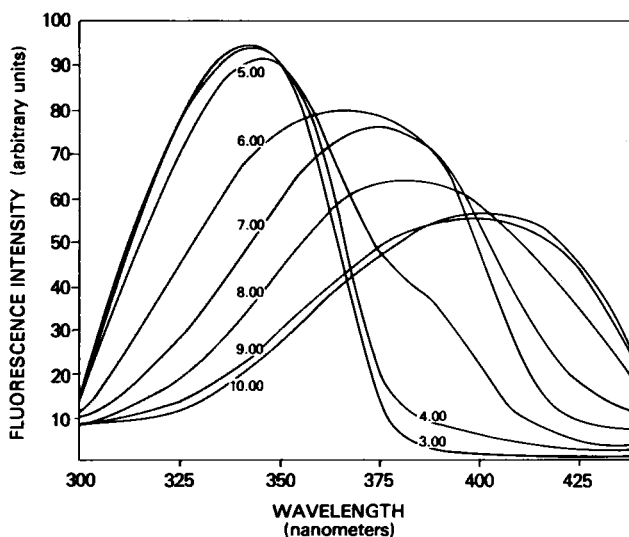

FIGURE 6 Excitation spectra (corrected) of 1,4-DHPN at various pH values; emission 470 nm. Note that there are three excitation peaks corresponding to the three forms of the probe; fully protonated, monoprotonated, and deprotonated forms. In the present study, the monoprotonated and deprotonated forms of 1,4-DHPN were excited with 375–407 nm light.
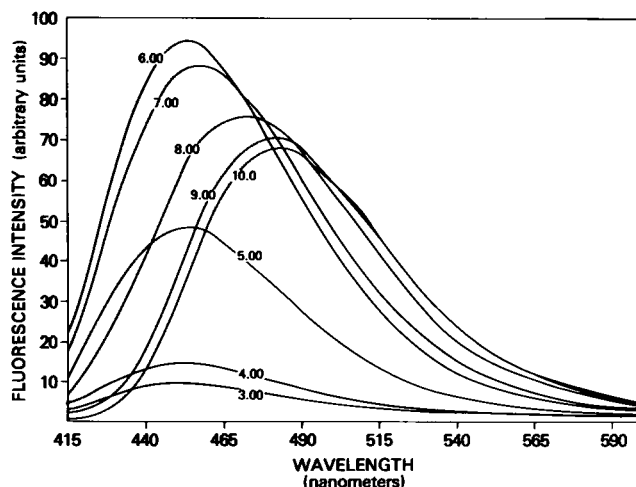
FIGURE 7 Emission spectra (corrected) of 1,4-DHPN at various pH values; excitation 386 nm. Note the shift in the emission peak from pH 6 to 10.

FIGURE 9 Optical titration curve of 1,4-DHPN using the microspectro-fluorometer (standards buffered with 10 mM HEPES and 10 mM Mes).

increased from 3 to 10 (excitation measured at 386 nm). The emission spectra were corrected for the spectral sensitivity of the photomultiplier detector. The shift in the emission peak is manifest as a change in fluorescence from blue to green as pH is increased. One can use the emission spectral shift to quantitate pH. By subtracting the emission spectrum obtained at pH 8.00 from the spectrum at pH 6.00 (the approximate range of pH_i to be measured within most cells), the two wavelengths where the fluorescence intensity changes most between these two pH values can be determined (Fig. 8). The fluorescence intensity at 512 nm increases with pH, whereas the fluorescence intensity at 455 nm decreases with pH. The ratio of the intensity at 512 nm to the intensity at 455 nm measured simultaneously is determined by the pH of the solution. By determining this ratio at various pH values using the microspectrofluorom-eter, an in vitro calibration curve (Fig. 9) was constructed.

The curve was not altered by varying Na^+ (20–130 mM), K^+ (30–130 mM), Ca^{++} (0–1 mM), Mg^{++} (0–1 mM). PO_4^{-3} (0–10 mM), and albumin (0–10 g/l).

Comparison of Spectra Obtained from A6 Cells and In Vitro Standards

To determine whether the intracellular environment of the probe 1,4-DPHN is similar to the in vitro standards, emission spectra obtained from the intracellular probe were compared with spectra obtained from in vitro standards. Since the intensity of each spectrum will vary with the amount of 1,4-DHPN being scanned (a factor that cannot be controlled in the cell), a method was devised to permit the comparison of spectral shape despite marked differences in fluorescence intensity. Fig. 10 is an emission spectrum obtained from intracellular 1,4-DHPN at an external pH of 7.6. Fig. 11 is a spectrum obtained from 1,4-DHPN in an in vitro standard, pH 7.51. Note the marked difference in total intensity precluding simple subtraction of the spectra as a method for comparing spectral shape. In order to scale the spectra without altering the spectral shape, an arbitrary wavelength was
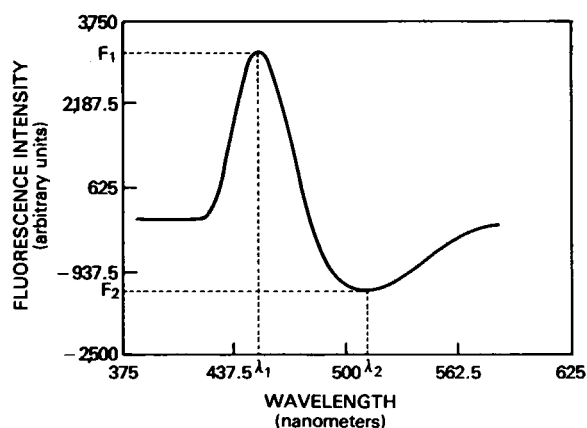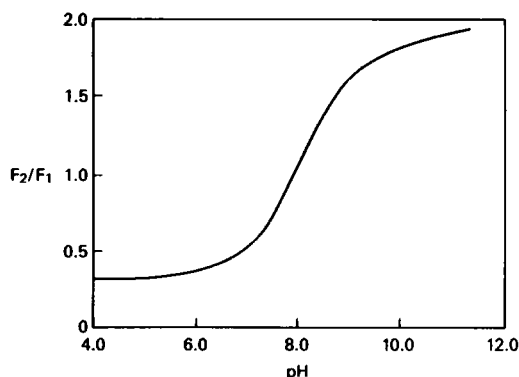

FIGURE 8 Subtraction of the emission spectrum obtained from a standard at pH 8, from the spectrum of a standard at pH 6 measured with the microspectrofluorometer. λ_1 and λ_2 are the two wavelengths where the maximum difference is found between these two spectra.
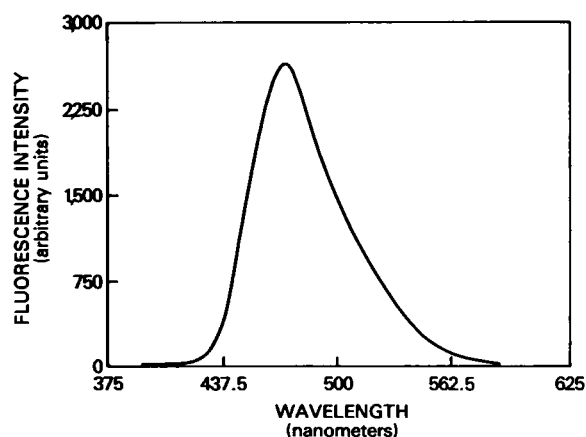

FIGURE 10 Emission spectrum obtained from intercellular 1,4-DHPN (external pH 7.6).
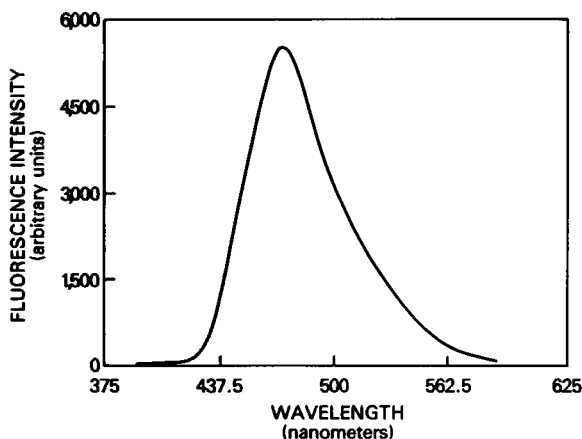
FIGURE 11 Emission spectrum obtained from 1,4-DHPN in a HEPES buffered standard, pH 7.51.
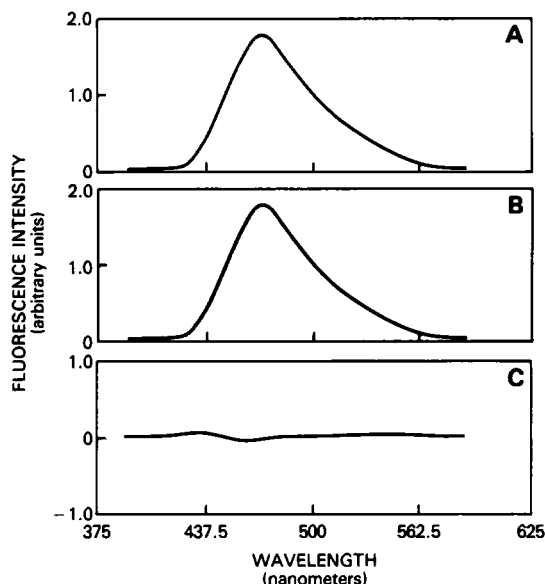

FIGURE 12 (*A*) Scaled emission spectrum of intracellular 1,4-DHPN. (*B*) Scaled emission spectrum of 1,4-DHPN, HEPES buffered standard, pH 7.51. (*C*) Subtraction of the scaled emission spectra indicates that the shape of the emission spectra in Fig. 10 and Fig. 11 are identical (within 4%).

chosen (455 nm), and the intensity at this wavelength was divided into the fluorescence intensity of all wavelengths for both spectra. Figs. 12 *A, B* are the scaled emission spectra from intracellular 1,4-DHPN and a standard pH 7.51, respectively. Subtraction of the two scaled spectra (Fig. 12 *C*) reveals that their intensity-compensated spectral shapes are identical, therefore, the intracellular environment did not alter the spectrum of the probe independent of pH. This indicates that an in vitro pH calibration curve can be used to calculate intracellular pH from in vivo measurements in A6 cells without requiring an indirect calibration procedure.

The Fluorescence Intensity Ratio Determined by Emission Spectroscopy

Emission spectroscopy permits the simultaneous measurement of two or more fluorescence intensities as opposed to fluorescence excitation spectroscopy where the fluorescence intensities must be measured at different times. The ratio of two fluorescent intensities measured simultaneously is less likely to be affected by bleaching, dye leakage out of the cell, and fluctuation in the intensity of the excitation source. In addition, since the entire spectrum is collected the bandwith of each of the two fluorescent intensities used in the ratio measurement can be precisely controlled and varied. Finally, emission spectroscopy permits the simultaneous measurement of spectra from multiple intracellular fluorescent probes provided each dye's respective emission spectrum is sufficiently different. The results in Table I demonstrate that despite a fourfold change in the concentration of 1,4-DHPN (in vitro standard pH 6.81) the fluorescence ratio remains 0.48. The precision of the measurement was determined by obtaining repeat measurements of the same in vitro standard, pH 7.00 The mean of eight determinations was 0.65 ± 0.002. The coefficient of variation was 0.83%.

Fig. 13 illustrates the results obtained during steady state pH$_i$ measurement in A6 cells loaded with 1,4-DHPN

(external pH 7.6). As a result of dye leakage and bleaching, the absolute intensity at 455 and 512 nm decreased with time. Fluctuation in the xenon arc lamp intensity caused the increase in the fluorescence intensity at 8.5 min. The ratio of the two intensities remained constant, compensating for these effects (Fig. 14). At external pH 7.6, the mean steady state pH$_i$ in A6 cells was 7.49 ± 0.04 (*n* = 12).

Regulation of pH$_i$ during Acute Acid and Alkali Loading

Existence of a pH$_i$ regulating mechanism in A6 cells was further suggested by the response of the cells to acute acid loading with a CO_2/HCO_3^- buffered solution (Fig. 15). The control pH$_i$ was monitored in a HEPES buffered solution at pH 7.6. The bathing solution was then changed

TABLE I
EFFECT OF CHANGING 1,4-DHPN
CONCENTRATION ON THE FLUORESCENCE
RATIO F_2/F_1 OF A STANDARD, pH 6.81*

pH	1,4-DHPN	F_1	F_2	F_2/F_1
	mM	*arbitrary units*		
6.81	0.05	14,429	6,919	0.480
6.81	0.033	11,859	5,713	0.482
6.81	0.025	9,550	4,607	0.482
6.81	0.017	5,074	2,426	0.478
6.81	0.0125	1,225	589	0.481

*Note the constancy of the F_2/F_1 ratio despite changes in the absolute fluorescent intensity value.
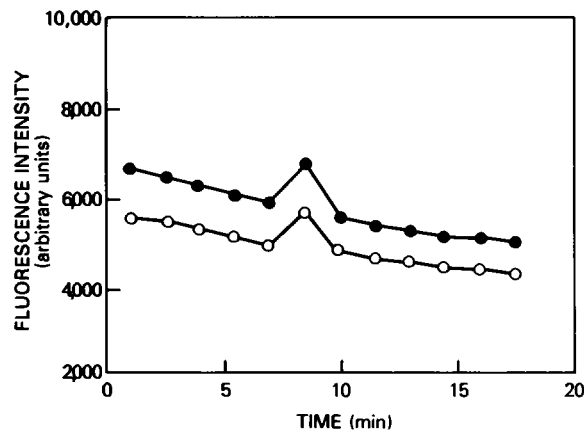
FIGURE 13 Absolute fluorescence intensity of F_1 (●——●) and F_2 (O——O) during steady state pH$_i$ measurement in A6 cells stained with 1,4-DAPN (bathing solution 10 mM HEPES, pH 7.6). Note (a) the decrease in intensity of F_1 and F_2 with time due to dye leakage and bleaching; (b) the fluctuation in the intensity of the excitation source (xenon light source) caused the increase in the intensity of F_1 and F_2 at 8.5 min.

to a solution containing 8 mM HCO_3^- equilibrated with 1% CO_2, pH 7.6. pH$_i$ decreased abruptly as a result of the rapid entry of CO_2 into the cells. On the continued exposure to the same solution, pH$_i$ recovered almost completely. Changing the bathing solution to the original HEPES containing solution at pH 7.6 resulted in an increase in pH$_i$ as a result of the rapid diffusion of CO_2 out of cells, and subsequent recovery. The ability of A6 cells to regulate pH$_i$ was also observed after acute acid loading following a brief exposure to 10 mM NH_4Cl. The pH$_i$ recovered exponentially to the control value after ~11 min (results not shown).

PH$_i$ Response to Changes in External pH

In addition to observing a pH$_i$ regulatory response during acute acid and alkali loads, the ability of A6 cells to maintain pH$_i$ was studied in response to steady state
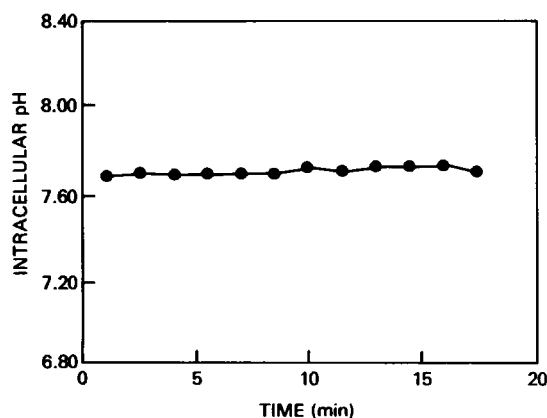

FIGURE 14 Steady state pH$_i$ calculated from ratio F_2/F_1. The ratio of the two fluorescence intensities measured simultaneously corrects for dye leakage, bleaching, and fluctuations in the excitation source.
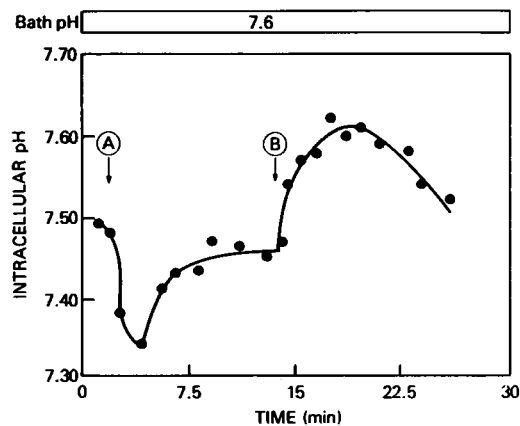

FIGURE 15 Regulation of pH$_i$ in A6 cells. A6 cells were bathed in 10 mM HEPES, pH 7.6. At A the bathing solution was changed to 8 mM $HCO_3^-/1\%$ CO_2, pH 7.6. Note the immediate fall in pH$_i$ as CO_2 enters the cell. pH$_i$ subsequently recovered almost completely as the intracellular $[HCO_3^-]$ increases. At B the bathing solution was changed to 10 mM HEPES, pH 7.6. Note that the alkaline overshoot and recovery of pH$_i$.

changes in the external pH (Fig. 16). pH$_i$ was monitored in A6 cells exposed for ~15 min (time to achieve new steady state pH$_i$) to HEPES buffered solutions at various external pH values (range 6.5–8.5). pH$_i$ remained relatively independent of the external pH.

Toxicity and Compartmentation of 1,4-DAPN/1,4-DHPN

The possible toxicity of 1,4-DAPN/1,4-DHPN to A6 cells was assessed by monitoring oxygen consumption as a index of mitochondria function, short circuit current as an index of active ion transport, and the morphology of the stained and unstained cells. The mean oxygen consumption of unstained A6 cell suspensions was 5.43 ± 0.06 nmol/mg/min ($n = 3$). The oxygen consumption of stained A6 cells (6.09 ± 0.22, $n = 4$) was not significantly different.
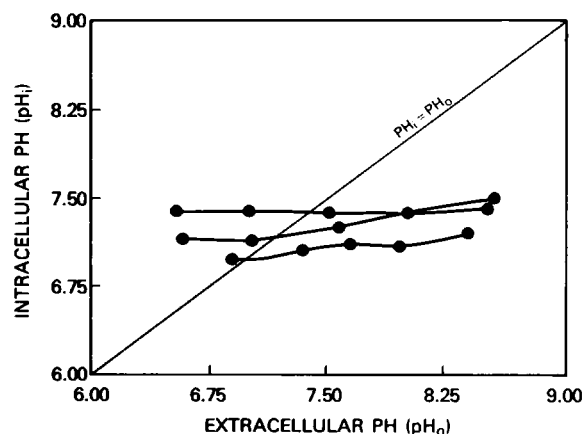

FIGURE 16 Effect of changes in extracellular pH (pH$_o$) on pH$_i$. A$_6$ cells were exposed to a given external pH (HEPES buffered) for 15 min (approximate time for pH$_i$ to reach state) after which pH$_i$ was measured. pH$_i$ remained relatively independent of pH$_o$ over a wide range of values.

The mean short circuit current was 38.5 ± 1.9 nA/5 cm^2 ($n = 4$) in unstained cells and was not significantly different one hour after staining (36.8 ± 3.8 nA/5cm^2; $n = 4$). Finally, the stained cells were not altered morphologically as accessed by differential interference contrast microscopy. In addition, the 1,4-DHPN fluorescence staining of the cells was diffuse throughout the cytosol and nucleus of the cells indicating that the dye was not significantly compartmentalized (Fig. 4). These results suggest that 1,4-DAPN and 1,4-DHPN are not toxic to these cells.

DISCUSSION

Several methods are currently available for monitoring pH$_i$ in living cells (1). Recently the use of trapped fluorescent probes to monitor pH$_i$ has become increasingly popular (3, 4). This method has several advantages over other techniques. (a) Fluorescence methods are essentially instantaneous permitting the tracking of acute change in pH$_i$, (b) the large signal-to-noise ratio permits the study of small numbers of cells, and (c) when studied with a microfluorometer, pH$_i$ can be monitored in single cells, tissues with various cell types, and cell monolayers.

Currently the most widely used fluorescent intracellular pH probe is 6-CF and its analogues (3–5). These probes all signal changes in pH$_i$ with a change in the intensity of a single emission peak. Unlike 6-CF and its analogues, 1,4-DHPN signals a change in pH with a shift in its peak emission wavelength. The fluorescence difference spectrum between an acid and alkaline solution of 1,4-DHPN has a maximum at 455 and a minimum at 512 nm. pH is then determined by calculating the ratio of the fluorescence intensity measurement at these two emission wavelengths. Since the two intensities are measured simultaneously, the measurement is independent of probe leakage out of the cell, bleaching, and fluctuation in the intensity of the excitation source. This is useful in a microfluorometer where repeated measurements are made on a single cell or small number of cells, which can result in a high bleaching rate. Another advantage of 1,4-DHPN is that pH can be determined using a single excitation bandwidth. The acid and base forms of 1,4-DHPN have distinct excitation peaks, therefore, it is useful to use a broad band excitation source as was done in the present study to maximally excite both forms of the probe simultaneously. However because the excitation spectrum of the acid and base forms of the probe overlap, excitation can also be performed successfully using a single wavelength source set at ~385 nm (Kurtz, I., and S. Balaban, unpublished results).[1]

While only two fluorescent intensity measurements are required to calculate pH$_i$, complete emission spectra (~500 intensity measurements) were collected from intracellular 1,4-DHPN. Analysis of emission spectra obtained from

intracellular probes permits the detection of light scattering, intracellular solvent polarity effects, intracellular binding, and chemical modification of the probe. In addition the spectral properties of a trapped intracellular probe can be altered by compounds that the cell is exposed to during the course of an experiment. When the fluorescence intensity ratio between two wavelengths is used to monitor pH$_i$, the calculated fluorescence intensity ratio could be altered without a change in pH occurring. Unless the spectral change is detected, the change in the fluorescence intensity ratio will be misinterpreted as a change in pH$_i$

The in vitro fluorescence spectrum and optical titration curve of 1,4-DHPN is insensitive to changes in Na$^+$, K$^+$, Ca^{++}, Mg^{++}, PO$_4^{-3}$ and albumin confirming that changes in the fluorescence intensity ratio of this compound are specific for pH. The emission spectra obtained from A6 cells loaded with 1,4-DHPN are identical to in vitro standards under the conditions of this study. This indicates that the intracellular environment is not altering the spectral characteristics of 1,4-DHPN making it possible to use an in vitro calibration curve to quantitate pH$_i$. Similar results have been obtained in MDCK cells. These findings may not pertain to all cell types. Indeed, in the proximal straight tubule of the rabbit kidney, which is capable of numerous chemical modification reactions (18), the spectrum of the probe was red shifted and altered in shape.

In all of the cell types investigated to date no visual compartmentation of the probe has been observed as presented in Fig. 4 for the A6 cells. The probe reports the cellular pH as an average of the cytosol and nucleus, with no observed difference in the nuclear and cytoplasmic pH.

In the present study, emission spectra were collected by focusing the fluorescence from living cells onto the entrance slit of an imaging monochromator, which was scanned by a SIT camera. The advantage of a multichannel detector system for collecting fluorescence emission and absorption spectra from in vitro and in vivo preparations is supported by several recent reports (19–24). In the present study, the SIT camera was used as a one-dimensional detector since in the data analysis, the pixel intensities along each channel were summed, resulting in a single intensity value per channel. The instrument can also be configured so that the spatial information provided by a two-dimensional detector is not sacrificed (19, 20, 24). This would be advantageous for applications where it is necessary to monitor fluorescent intensities originating from discrete regions of a cell (e.g., in generating cellular maps of pH or other ions). A pH map of a cell can be generated using 1,4-DHPN by splitting the fluorescence with a 50:50 beamsplitter so that 50% of the fluorescence is imaged by an SIT camera through a 455-nm filter and 50% of the fluorescence is imaged by a second SIT camera through a 512-nm filter. After digitizing the two images simultaneously, substracting the respective dark current images and dividing one image by the other, a fluorescence intensity ratio (and therefore pH) can be obtained at every

---

[1]385 nm is the wavelength where the excitation spectrum of the partially protonated form and fully deprotonated form of 1,4-DHPN overlap maximally.

pixel of the digitized image. The advantage of using 1,4-DHPN to generate a pH map of the cell is that unlike fluorescein and its analogues (9), the images can be acquired simultaneously so that bleaching, dye leakage, and excitation source fluctuation are less likely to affect the ratio.

The mean steady state pH_i in A6 cells was 7.49 ± 0.04. The calculated equilibrium potential for H^+ (and OH^-) at an external pH of 7.6 is therefore −6.4 mV. Since the intracellular membrane potential of A6 cells is approximately −30 to −50 mV (R. Fisher, personal communication), the $[H^+]$ is being maintained above its electrochemical equilibrium.

The pattern of acidification and recovery observed in A6 cells on exposure to a CO_2/HCO_3^- containing solution has been observed in other cell types (8, 25–27). The initial fall in pH_i results from the rapid entry of CO_2 into the cell which combines with H_2O to generate H^+. The rise in pH_i after CO_2 removal and its subsequent recovery has also been observed in other cell types (8). The initial rise in pH_i is believed to be due to the rapid efflux of CO_2 from the cell. The recovery of pH_i following acute acid and base loading reflects the ability of A6 cells to regulate pH_i. The transport processes involved remain to be determined.

pH_i remained relatively constant despite large changes in external pH (Fig. 16). Similar results have been obtained in numerous cell types (28–31). This finding can be explained either by a low passive flux of H^+ or by a pH_i regulatory mechanism. Whatever the mechanism, A6 cells appear to be protected from large changes in environmental pH.

In summary, we have developed a new method for measuring pH_i in cultured cell monolayers using the fluorescent pH probe 1,4-DHPN. Because of the unique spectral properties of the probe, emission rather than excitation spectroscopy can be used to monitor pH. Emission spectroscopy permits the simultaneous measurement of two or more fluorescent intensities provided a probe demonstrates either: (a) distinct emission peaks in its bound and unbound form, (b) a shift in the peak emission wavelength of its bound and unbound form. In this study, pH_i was monitored in the A6 epithelial cell line and was found to be 7.49 ± 0.04 ($n = 12$) with an external pH of 7.6. The cells regulated pH_i in response to acute acid and alkali loading. In addition, pH_i was found to be relatively independent of the external pH over a wide range of values. 1,4-DHPN was not compartmentalized and was not toxic to these cells.

Several analogues of 1,4-DHPN have been synthesized, which demonstrate a spectral shift in the peak emission wavelength as pH changes, yet differ from the parent compound in their lipid solubility and pK values. These compounds will be discussed in greater detail in a later publication.

REFERENCES

1. Roos, A., and W. B. Boron. 1981. Intracellular pH. *Physiol. Rev.* 61:296–433.
2. Busa, W. B., and R. Nuccitelli. 1984. Metabolic regulation via intracellular pH. *Am. J. Physiol.* 15:R409–R438.
3. Thomas, J. A., R. N. Buchsbaum, A. Zimniak, and E. Racker. 1979. Intracellular pH measurements in Ehrlich acites tumor cells utilizing spectroscopic probes generated in situ. *Biochemistry.* 18:2210–2218.
4. Belt, J. A., J. A. Thomas, R. N. Buchsbaum, and E. Racker. 1981. Inhibition of lactate transport and glycolysis in Ehrlich acites tumor cells by bioflavinoids. *Biochemistry.* 18:3506–3511.
5. Rink, T. J., R. Y. Tsien, and T. Pozzan. 1982. Cytoplasmic pH and free Mg in lymphocytes. *J. Cell Biol.* 95:189–196.
6. Moolenaar, W. H., L. G. J. Tertoolen, and S. W. de Laat. 1984. The regulation of cytoplasmic pH in human fibroblasts. *J. Biol. Chem.* 259:7563–7569.
7. Heiple, J. M., and D. L. Taylor. 1980. Intracellular pH in single motile cells. *J. Cell Biol.* 86:885–890.
8. Rothenberg, P., L. Glaser, P. Schlesinger, and D. Cassel. 1983. Activation of Na/H exchange by epidermal growth factor elevates intracellular pH in A431 cells. *J. Biol. Chem.* 258:12644–12653.
9. Tanasugarn, L., P. McNeil, G. T. Reynolds, and D. L. Taylor. 1984. Microspectrofluorometry by digital image processing: Measurement of cytoplasmic pH. *J. Cell Biol.* 98:717–724.
10. Ohkuma, S., and B. Poole. 1978. Fluorescence probe measurements of the intralysosomal pH in living cells and the perturbation of pH by various agents. *Proc. Natl. Acad. Sci. USA.* 78:3327–3331.
11. Rogers, J., T. Hesketh, G. A. Smith, and J. C. Metcalfe. 1983. Intracellular pH of stimulated thymocytes measured with a new fluorescent indicator. *J. Biol. Chem.* 258:5994–5997.
12. Strzelecki, T., J. A. Thomas, C. D. Koch, and K. F. LaNoue. 1984. The effect of hormones on proton compartmentation in hepatocytes. *J. Biol. Chem.* 259:4122–4129.
13. Valet, G., A. Raffael, L. Moroder, E. Wunsch, and G. Ruhenstroth-Bauer. 1981. Fast intracellular pH determination in single cells by flow cytometry. *Naturwissenschaften.* 68:265–266.
14. Brown, R. G., and G. Porter. 1977. Effect of pH on the emission and absorption characteristics of 2,3-Dicyano-p-hydroquinone. *J. Chem. Soc. Faraday Trans. I.* 73:1281–1285.
15. Allen, C. F. H., and C. V. Wilson. 1941. The mechanism of addition of hydrogen cyanide to benzoquinone. *J. Am. Chem. Soc.* 63:1756.
16. Rafferty, K. A. 1963. *In* Biology of Amphibian Tumours. M. Mizell, editor. Springer-Verlag, New York. 52–81.
17. Wolfbeis, O. S., and E. Koller. 1983. Fluorometric assay of hydrolases at longwave excitation and emission wavelengths with new substrates possessing unique water solubility. *Anal. Biochem.* 129:365–370.
18. Endou, H., C. Koseki, S. Hasumura, K. Kakuno, K. Hojo, and F. Sakai. 1982. Renal cytochrome P450: Its localization along a single nephron and its induction. *In* Biochemistry of Kidney Functions. F. Morel, editor. Elsevier Biomedical Press, New York.
19. Talmi, Y., editor. 1983. Multichannel Image Detectors. American Chemical Society Symposium Series 236. Washington, D.C. 332 pp.
20. Olesik, J. W., and J. P. Walters. 1984. Characterization and use of the silicon intensified target vidicon detector in basic and applied research in atomic spectroscopy. *Appl. Spectrosc.* 38:578–585.
21. Mandel, L. J., T. G. Riddle, and J. C. Lamanna. 1976. A rapid scanning spectrophotometer and fluorometer for in vivo monitoring of steady-state and kinetic optical properties of respiratory enzymes. *In* Oxygen and Physiological Function. Frans Jobsis, editor. Professional Information Library, Dallas, TX. 79–89.
22. Balaban, R. S., S. P. Soltoff, J. M. Storey, and L. J. Mandel. 1980.

Improved renal cortical tubule suspension: spectrophotometric study of oxygen delivery. *Am. J. Physiol.* 238:F50–F59.

23. Balaban, R. S., and A. Sylvia. 1981. Spectrophotometric monitoring of oxygen delivery to the exposed rat kidney. *Am. J. Physiol.* 241:F257–F262.

24. Balaban, R. S., I. Kurtz, H. Cascio, and P. Smith. 1984. Topological spectral scanning of single cells. *J. Gen. Physiol.* 84:21a. (Abstr.)

25. Boron, W. F., and P. DeWeer. 1976. Intracellular pH transients in squid giant axons caused by CO_2, NH_3 and metabolis inhibitors. *J. Gen. Physiol.* 67:91–112.

26. Boron, W. F. 1977. Intracellular pH transients in giant barnacle muscle fibers. *Am. J. Physiol.* 233:C61–C73.

27. Thomas, R. C. 1976. The effect of carbon dioxide on the intracellular pH and buffering power of snail neurons. *J. Physiol. (Lond.).* 255:715–735.

28. Gilles, R. J., T. Ogino, R. G. Shulman, and D. C. Ward. 1982. ^{31}P NMR evidence for the regulation of intracellular pH by Ehrlich acites tumor cells. *J. Cell Biol.* 95:24–28.

29. Sanders, D., and C. C. Slaymen. 1982. Control of intracellular pH; Predominant role of oxidative metabolism, not proton transport in the eukaryotic microorganism *Neurospora. J. Gen Physiol.* 80:377–402.

30. Navon, G., R. G. Shulman, T. Yamane, T. R. Eccleshall, K. B. Lam, J. J. Baronofsky, and J. Marmur. 1979. ^{31}P nuclear magnetic resonance studies of wild type and glycolytic pathway mutants of *Saccharamyces cerevisiae. Biochem. J.* 18:4487–4499.

31. Slonizeweski, J. L., B. P. Rosen, J. R. Alger, and R. M. Macnab. 1981. pH homeostatsis in *Escherichia coli:* Measurement by ^{31}P NMR of methylphosphate and phosphate. *Proc. Natl. Acad. Sci. USA.* 78:6271–6275.